EXPERIMENTAL INVESTIGATION OF THERMAL PERFORMANCE AND ENTROPY ANALYSIS OF SPHERE TURBULATORS

Taha Resul KARAKUS [1], Ilker FIRAT [*2], Orhan YILDIRIM [1], Fatin SONMEZ [3], Sevinc Sevgi CICEK KOCALI [1], Abdussamed YILDIZ [1], Sendogan KARAGOZ [1], Omer COMAKLI [1]

[1] Department of Mechanical Engineering, Ataturk University, Erzurum, Turkey

[*2] Ilic Dursun Yildirim Vocational School, Erzincan Binali Yildirim University, Erzincan, Turkey

[3] Artvin Vocational School, Artvin Coruh University, Artvin, Turkey

[*] Corrresponding author; E-mail: ifirat@erzincan.edu.tr

In this study, the effects of different numbers of sphere turbulators placed in a circular-shaped test pipe under turbulent flow conditions on heat transfer, friction factor, thermal performance factor and entropy production were experimentally investigated. Water was used as the working fluid in the experiments carried out in the number range Re=8379-16701. Initially, plain pipe and supported plain pipe experiments were carried out by keeping the fluid inlet temperature and test pipe surface temperature constant. Then, 1, 2 and 3 sphere turbulator experiments were carried out under the same conditions, respectively. According to the findings, the maximum Nusselt number increase compared to the supported plain pipe was 83.34% for the test pipe with 3 sphere turbulators. The minimum and maximum Nu number increase rates of 3 sphere turbulators compared to 1 and 2 sphere turbulators were obtained as 42.61%-46.93% and 13.99%-17.11%, respectively. The increase rates of maximum friction factors of 1, 2 and 3 sphere turbulators compared to the supported plain pipe were 174.42%, 226.70% and 306.53%, respectively. In addition, the maximum total entropy rate for sphere turbulators was obtained as 0.058 $W.m^{-1}.K^{-1}$ for 1 sphere turbulator at Re = 8379. In terms of the second law, the maximum entropy generation of sphere turbulators compared to the supported plain pipe decreased by 79.39% for 3 sphere turbulators at Re = 8379. As a result, it was concluded that the optimum number of sphere turbulators is 3 sphere turbulators with the lowest entropy production number and the highest TPF value (1.28).

Key words: turbulator, entropy, thermal performance, Reynolds number

1. Introduction

These days, heat exchange equipment is essential to many different sectors. Heat exchangers are equipment used to transfer thermal energy between two or more fluids separated by solid matter. Improving heat exchangers' thermal efficiency is crucial for reducing energy and material usage [1].

Heat exchangers; it is used in industries to crystallize, concentrate, distill, fractionate, pasteurize, sterilize and control a process fluid. It is also widely used in some heat exchangers, cooling towers, evaporators, automobile radiators, air preheaters, condensers, shell and tube exchangers [2,3].

In heat exchangers, there are two ways to raise the intensity of the heat transfer rate: passive and active. When using passive methods, heat transfer is increased without the usage of external energy. The thermal boundary layer is affected, for instance, by modifications to tube geometry [4,5], the use of nanofluids [6-8], or the positioning of turbulators in the heat exchanger tube in different configurations to disrupt the flow [9].

Turbulators are commonly used in heat exchangers to improve heat transfer by altering fluid flow and increasing forced convection. Turbulators come in different shapes and geometries that can be used in other applications for various flow regimes [10].

The impact of a three-blade vortex generator on the second law performance of a tube heat exchanger outfitted with the aforementioned accessories was documented by Bahuguna *et al.* [11]. Their conclusion was that the entropy produced as a consequence of heat transfer is far higher than the entropy produced as a result of the friction factor.

Maithani and Kumar [12] investigated the effects of a heat exchanger tube with dimpled ribs on its inner wall on pressure drop and heat transmission in their experimental investigation. They looked into the effects of geometric characteristics, primarily the ratio of printing diameter to dimple depth, the spacing in the span direction, and the spacing in the flow direction. The flow wise spacing (x/d_d) and aperture spacing (y/d_d) of the heat exchanger tube are both within the same range. Similarly, the Reynolds number (*Re*) runs from 5000 to 27000, and the dimpled depth to printing diameter ratio (e/d_d) is within the same range of 0.5–1.5. The testing results showed that the thermal hydraulic performance and heat transfer increased by 2.53 times and 4.19 times, respectively, using x/d_d 15, y/d_d 15, and e/d_d 1.0.

The performance of systems decreases as exergy destruction, which is a result of entropy formation, increases [13]. Therefore, entropy analysis is vital. The study of innovative turbulators together in terms of entropy generation and heat transfer has recently attracted the attention of researchers.

Sepehr et al.'s study [14] used numerical analysis to look at entropy production, pressure loss, and heat transfer in shell and coiled tube heat exchangers. Consequently, they put out a few correlations for calculating the friction factor (*f*) and the Nusselt number (*Nu*) on the shell side. They also obtained a relationship between NTU, entropy production rate and thermal efficiency. They also obtained a relationship between NTU, entropy production rate and thermal efficiency.

In their study, Gord *et al.* [15] aimed to find the optimum geometry and operating conditions of spiral wound heat exchangers for both laminar and turbulent flows, based on the second law of thermodynamics. As a result, taking into account the applied numerical simulation results, optimum geometry and flow properties were determined that optimized the heat exchanger's efficiency examined based on the lowest entropy production rate.

In addition to the above studies, many studies have recently been carried out in the literature to increase heat transfer and thermal performance with new types of inserts placed in the test pipe in channels and pipes with different geometric shapes [16-22].

The aim of this study is to determine the optimum number of sphere turbulators that provide maximum thermal performance of a heat exchanger tube, taking into account the first and second laws

of thermodynamics. For this reason, the effects of different numbers of sphere turbulators placed in a circular shaped exchanger pipe on heat transfer, friction factor, thermal performance factor, heat and viscose-induced irreversibilities and entropy production and total entropy production number in the 8379-16701 Reynolds number range were experimentally investigated.

2. Material Method

2.1. The experimental setup

The picture view and schematic view of the experimental setup are given in Figs. 1 and 2, respectively. Additionally, detailed information about the experimental setup equipment and the execution of the experiment is explained in reference [23]. Water was used as the working fluid. The test pipe's surface temperature was measured using eighteen T-type thermocouples.

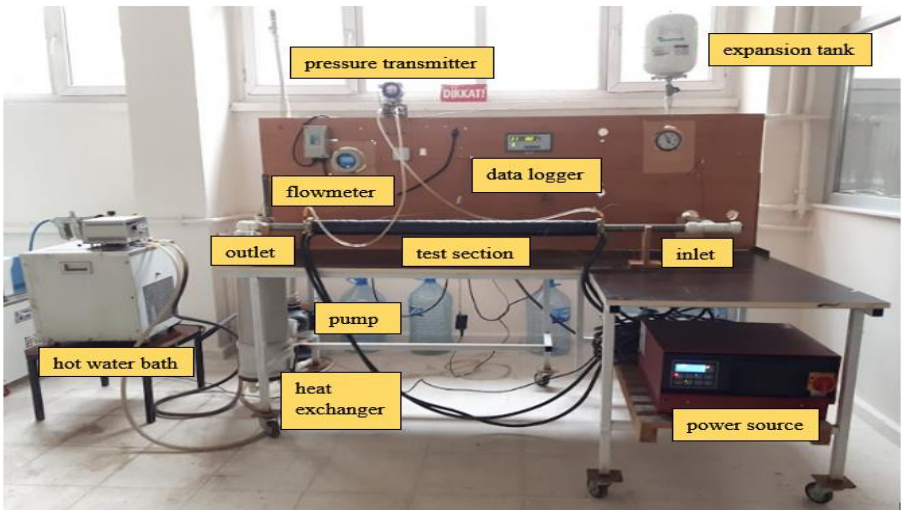

Figure 1. Picture view of the experimental setup

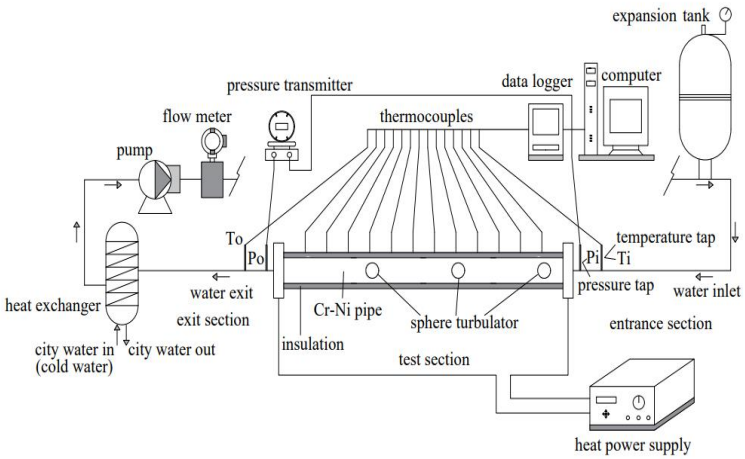

Figure 2. Schematic view of the experimental setup

The entrance temperature of the fluid to the test section was kept constant at 25 $^{\circ}$C. Thanks to the power supply, a constant and continuous 488.04 W (294 A and 1.66 V) heat was provided to the test pipe. Experiments were carried out at six different fluid flow rates (1000 L.h^{-1}, 900 L.h^{-1}, 800 L.h^{-1}, 700 L.h^{-1}, 600 L.h^{-1} and 500 L.h^{-1}) and in the range *Re*=8379-16701.

2.2. Turbulator and Support Element

A 0.002 m diameter straight wire rod was positioned parallel to the axis of the test tube's circular form. Sphere turbulators are fixed on this wire rod at specified distances and in different numbers (1, 2 and 3 pieces). In addition, support elements were positioned on the wire rod to ensure that the wire and sphere turbulators remained in the pipe axis during the experiments. Support elements and sphere turbulators were manufactured on a 3D printer. The test section is shown

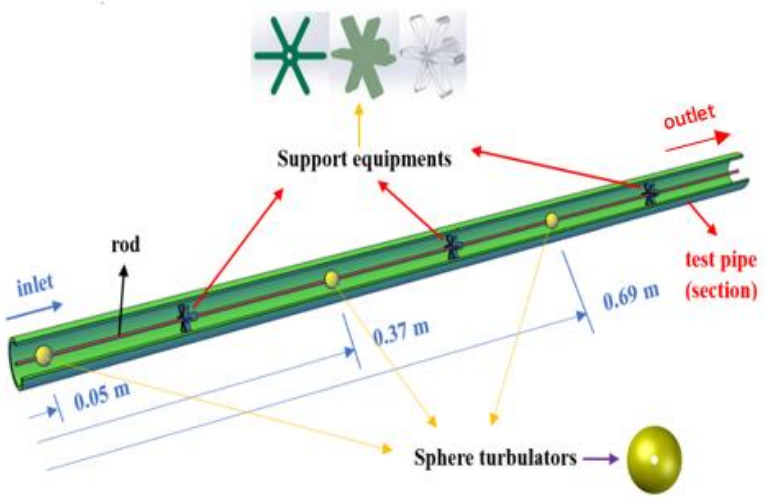

schematically in Fig. 3.

Figure 3. The test section's schematic view

A close-up of the spherical turbulators and support components installed in the test pipe is shown in Fig. 3. The diameter of the sphere turbulator is 0.0156 m, and a hole is drilled in the middle for a wire rod with a diameter of 0.002 m. The height of the support elements is equal to the inner diameter of the test pipe (0.02552 m) and the support elements are placed at an equal distance from the sphere turbulators. At first, plain pipe experiments were conducted. Later, studies with support equipments were conducted. Since the positions and numbers of support elements did not change in all sphere turbulator experiments, the pipe with support elements was accepted as an plain pipe. After the pipe experiments with 1 sphere turbulator, experiments were carried out with 2 and 3 turbulators, respectively.

2.3. Data Reduction

For the steady state of the convective heat transfer rate, the heat provided to the pipe by the power source is assumed to be equal to the heat transferred from the pipe to the fluid and is calculated with Eq. (1) [24].

$$Q_w = Q_{conv} \tag{1}$$

$$Q_w = \dot{m} C_{p,w} (T_o - T_i) \tag{2}$$

$$Q_{conv} = hA(T_{m,avg} - T_{w,avg}) \tag{3}$$

Here Q_w; is the amount of heat supplied to the test pipe, while Q_{conv} [W] indicates the rate of heat transfer by convection. $\dot{m}$[kg.sec^{-1}], $C_{\mathrm{p,w}}$[kj.kg^{-1} .K^{-1}], T_o[K], T_i[K], h[W.m^{-2}.K^{-1}], A[m^2], $T_{\mathrm{m,avg}}$[K] and $T_{\mathrm{w,avg}}$[K] symbolizes the mass flow rate, specific heat at constant pressure, exiting fluid temperature, entering fluid temperature, heat transfer coefficient, average temperature of the fluid and average temperature of the pipe wall, respectively.

$T_{\mathrm{m,avg}}$[K] was calculated by taking the average of the inlet and outlet temperature of the fluid and using Eq. (4).

$$T_{m,avg} = \frac{T_i + T_o}{2} \tag{4}$$

Using Eq. (5), the average local surface temperatures of eighteen evenly spaced sites from the test pipe's entrance to its exit were used to determine $T_{\mathrm{w,avg}}$.

$$\boldsymbol{T_{w,avg} = \sum_{1}^{18} \frac{T_w}{18}} \tag{5}$$

Losses occurring in a heat exchanger; it is caused by heat exchange due to finite temperature difference, friction and heat exchange with the environment. Since the test pipe was insulated, heat losses to the environment were neglected. Entropy production in a heat exchanger is calculated as follows [23].

$$\boldsymbol{\dot{S}'_{gen,total} = \dot{S}'_{gen,ht} + \dot{S}'_{gen,ff} = q'^2/(\pi k T_b{}^2 Nu) + 32\dot{m}^3 f/(\pi^2 \rho^2 T_b D_h{}^5)} \tag{6}$$

$\dot{S}'_{\mathrm{gen,total}}$ [W.m^{-1}.K^{-1}]; total entropy production, $\dot{S}'_{\mathrm{gen,ht}}$ [W.m^{-1}.K^{-1}]; heat transfer and $\dot{S}'_{\mathrm{gen,ff}}$ [W.m^{-1}.K^{-1}] symbolize the entropy formation related to friction irreversibility. q' [W.m^{-1}]; heat transfer per unit length, ρ [kg.m^{-3}]; fluid density, k [W.m^{-1}.K^{-1}]; heat conduction coefficient, D_{h} (m); represents the hydraulic diameter.

Eq. (7) yields the dimensionless total entropy production number N_{s} [25].

$$\boldsymbol{N_s = \frac{\dot{S}'_{gen,total}}{k}} \tag{7}$$

Eq. (8) gives the expression for the experimental friction factor (*f*) [26].

$$\boldsymbol{f = \frac{2\Delta p D_h}{\rho u^2 L}} \tag{8}$$

Eq. (9) determines the dimensionless *Re*.

$$\boldsymbol{Re = \frac{\rho u D_h}{\mu}} \tag{9}$$

The fluid velocity is represented by u [m.s^{-1}] and the dynamic viscosity by μ [kg.m^{-1}.s^{-1}]. *Nu* was computed using Eq. (10).

$$\boldsymbol{Nu = \frac{h D_h}{k}} \tag{10}$$

The thermal performance of sphere turbulators was determined by comparing the turbulator pipe with the supported empty pipe under equal pumping power. Eq. (11) illustrates equal pumping power.

$$\boldsymbol{(\dot{Q}\Delta p)_a = (\dot{Q}\Delta p)_o} \tag{11}$$

The pressure drop is shown here by Δp (Pa), volumetric flow rate, and $\dot{Q}$ [m^3.h^{-1}]. The connection between the *f* and *Re* is given by Eq. (12).

$$\boldsymbol{(f Re^3)_a = (f Re^3)_o} \tag{12}$$

TPF of sphere turbulators was found with Eq. (13).

$$TPF = \frac{h_a}{h_o}\Big|_{pp} = \frac{Nu_a}{Nu_o}\Big|_{pp} = \frac{\frac{Nu_a}{Nu_o}}{\left(\frac{f_a}{f_o}\right)^{1/3}} \tag{13}$$

The thermal performance factor was calculated at the same pumping power using the Nusselt number (Nu_a) and friction factor (f_a) of the turbulated pipe and the Nusselt number (Nu_o) and friction factor (f_o) of the supported empty pipe [26,27].

The correctness of the results of the experiment was checked using the Kline [28] approach.

$$\Delta R = \sqrt{\sum_{j=1}^{M} \left(\frac{\partial R}{\partial X_j}\Delta X_j\right)^2} \tag{14}$$

The uncertainty pertaining to the independent and dependent variables are denoted by δX_j and δR in Eq. (14). j is the specific parameter counter, and M is the number of arguments. The temperature readings of the fluid at the test pipe's entrance and exit, pressure readings, and inlet velocity readings are the primary factors identified in the error analysis.

Uncertainties about the values found in the course of experimental research employing Eq. (14); it was calculated as 4.86% for Nusselt number, 1.77% for Reynolds number and 2.55% for friction factor. Additionally, the uncertainties of other parameters are given in Tab. 1.

Table 1. Uncertainties in measured and calculated parameters

Parameter	Uncertainty
Temperature, Data logger	±%0.5
Pressure transmitter, Flowmeter	±%0.1
Power source	±%0.2

3. Results and discussion

3.1. Validation experiments

Before examining the effects of sphere turbulators, validation was done with valid correlations in the literature. For this purpose, graphic curves were obtained by calculating the experimentally obtained Nusselt number and friction factor values for the empty pipe. These graphs are compared to the Petukhov correlation for heat transfer and the Blasius correlation for friction. In the case of fully developed turbulent flow in an empty pipe, Petukhov and Blasius correlations are given in Eq. (15) [29] and Eq. (16) [30,31], respectively.

$$Nu = \frac{\left(\frac{f}{8}\right)RePr}{1.07+12.7\left(\frac{f}{8}\right)^{\frac{1}{2}}\left(Pr^{2/3}-1\right)} \qquad \text{for} \quad 10^4 < Re < 5\text{x}10^6 \tag{15}$$

$$f = 0.316Re^{-0.25} \qquad \text{for} \quad Re \leq 2\text{x}10^5 \tag{16}$$

Comparison of heat transfer and friction factor graphs obtained from empty pipe experimental results [32] with correlations in the literature is given in Fig. 4.

According to Fig. 4, the experimental results of the Nusselt numbers and friction factor of the empty pipe are in agreement with the study [33] and correlations found in the literature. The maximum error between experimental data and Petukhov correlation was calculated as 7.78%. Since the Blasius correlation is valid for frictionless internal flows and the friction factor of each pipe used in industry is different, it must be found by experimental methods. For increasing Reynolds numbers, the Nu values of the plain pipe increased, while the friction factor values decreased. Since every pipe used in industry has a distinct friction factor and the Blasius correlation only holds true for frictionless internal flows, it must be determined by experimental methods [32].

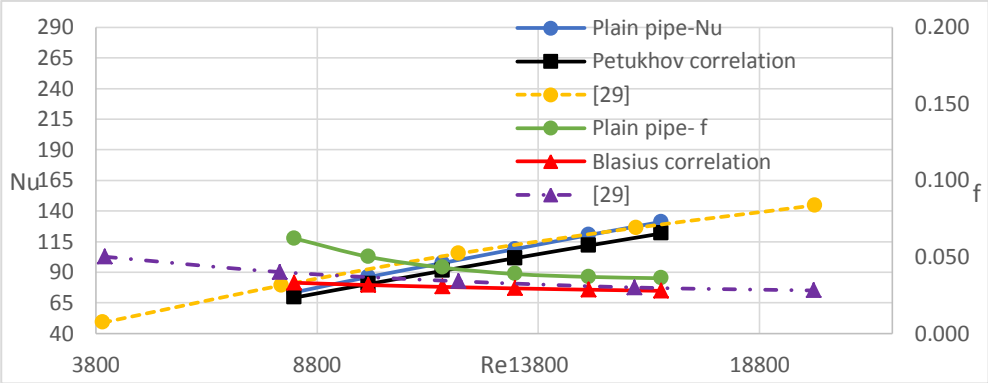

Figure 4. Comparison of *Nu-Re* and *f-Re* graphs of the plain pipe with the literature

3.2. Effects of sphere turbulators on heat transfer, friction factor and thermal performance factor

Since different numbers of sphere turbulators placed in the test pipe create obstacles to the flow and increase the turbulence of the flow, their effects on heat transfer, friction factor and their combination, the thermal performance factor (*TPF*), occur. Fig. 5 shows the effects of different numbers of sphere turbulators on heat transfer graphically.

According to Fig. 5, as the number of sphere turbulators increases, *Nu* values also increase. Additionally, with the increase in Reynolds number, Nusselt number values increased. Nusselt number values for all sphere turbulators were obtained on the supported empty pipe. The minimum and maximum increases in Nusselt numbers of 1, 2 and 3 sphere turbulators compared to the supported empty pipe are 20.17%-25.39%, respectively; 51.52%-56.55%; it was realized as 74.48%-83.34%. The *Nu* increase rates of 3 sphere turbulators compared to 1 and 2 sphere turbulators were 42.61%-46.93% and 13.99%-17.11%, respectively. The increasing number of sphere turbulators in the test pipe increased the turbulence of the fluid and enabled it to come into greater contact with the wall. Due to the increasing number of turbulators, the residence time of the fluid in the test pipe was prolonged. For this reason, Nusselt number values increased due to the increase in the fluid temperature difference between the test pipe inlet and outlet.

Fig. 6 shows the effects of different numbers of sphere turbulators on the friction factor.

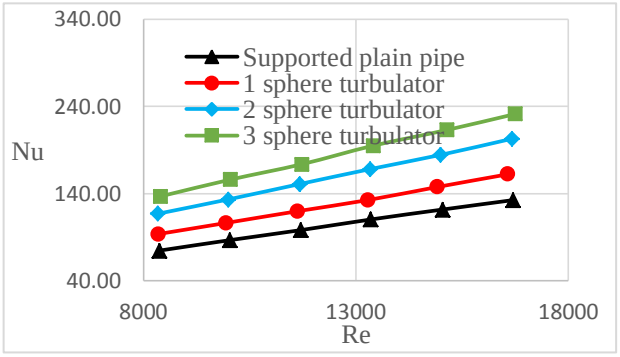

Figure 5. *Nu-Re* graph of different numbers of sphere turbulators

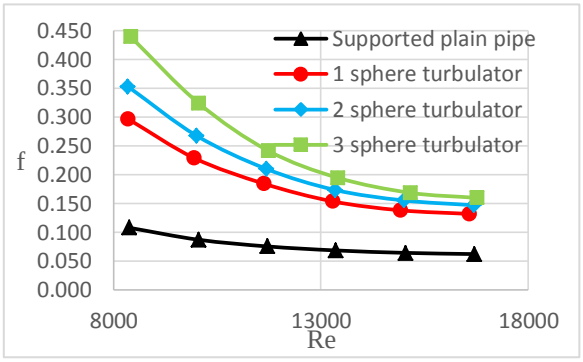

Figure 6. *f-Re* graph of different numbers of sphere turbulators

According to Fig. 6, friction factor values for sphere turbulators were obtained on the supported empty pipe in all cases. Additionally, the friction factor decreased with increasing *Re*. In comparison to the supported empty pipe, the rise rates of the friction factors of the 1, 2, and 3 sphere turbulators were 111.49%–174.42 percent, 135.59%–226.70%, and 156.07%–306.53%, respectively. Increasing the number of sphere turbulators increased the friction factor due to the increase in the pressure drop between the inlet and outlet of the test pipe.

The effects of sphere turbulators on the thermal performance factor (*TPF*) calculated with Eq. (13) are given in Fig. 7.

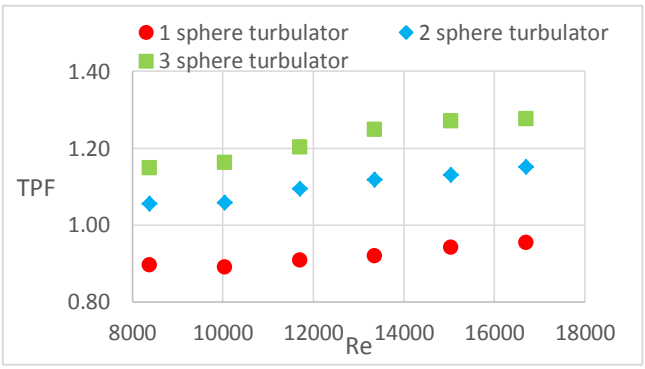

Figure 7. *TPF-Re* chart of sphere turbulators

According to Fig. 7, the thermal performance factors of sphere turbulators compared to the supported empty pipe are above 1 except for one sphere turbulator. This shows that for 1 sphere turbulator, the friction factor is more dominant than heat transfer, and for 2 and 3 sphere turbulators, heat transfer is effective from the *f*. According to the *TPF* values calculated from the test data, the order from maximum *TPF* value to minimum *TPF* value is determined as $TPF_3 > TPF_2 > TPF_1$. Lowest *TPF* value; while it was 0.89 in 1 sphere turbulator at *Re*=10043, the highest TPF value was obtained as 1.28 in 3 sphere turbulators for *Re*=16701. It has been observed that *TPF* values increase with increasing Reynolds number.

To evaluate the thermal performances of different numbers of sphere turbulators, comparisons were made with the literature and are presented in Tab. 2.

Table 2. Comparison of the current study with the literature in terms of thermal performance

Author(s)	Turbulator type	*Re*	Maksimum *TPF*
Luo *et al.* [34]	the special shape twisted tape and helical coil wire turbulator	5000-9000	1.31
Hong *et al.* [35]	multiple twisted tapes	5800-19200	0.94
Kongkaitpaiboon *et al.* [36]	perforated conical-rings	4000-20000	0.92
Eiamsa-ard *et al.* [37]	short length twisted tape	4000-20000	1.00
Present study	sphere turbulators	16701	1.28

Tab. 2 presents the findings, which indicate that the thermal performances of various spherical turbulators studied experimentally were often greater than those of comparable research in the literature.

3.3. Second law analysis

Different numbers of sphere turbulators were examined in terms of their thermal performance as well as the second law of thermodynamics. Entropy production rates associated with heat transport and frictional irreversibilities were calculated for this purpose.

In the number range *Re* = 8379–16701, the entropy production associated with heat transfer and friction irreversibilities induced by supported plain tube and spherical turbulators is depicted in Fig. 8.

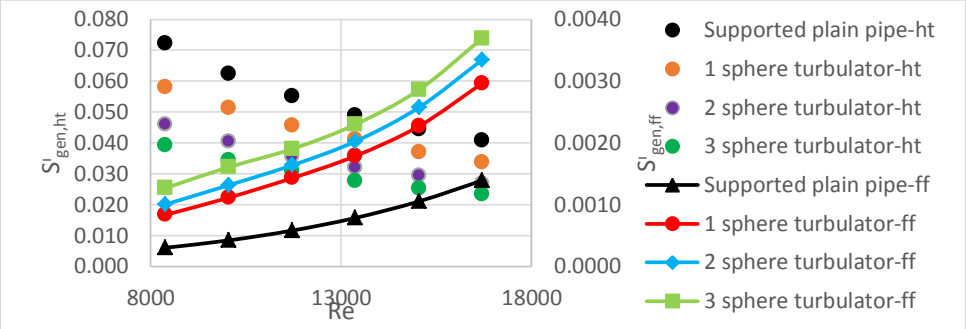

Figure 8. $S'_{gen,ht}$-*Re* and $S'_{gen,ff}$-*Re* graphs of supported empty pipe and sphere turbulators

According to Fig. 8, as the Reynolds number increases due to increasing fluid flow rate, the entropy production rate due to heat transfer decreases, while the entropy production rate due to viscous increases. Moreover, the temperature differential between the fluid and the pipe inner wall decreased as a result of the rise in fluid flow rate. These explanations explain why, as fluid velocity increased, entropy production resulting from irreversible heat transfer decreased [38]. The test pipe's employment of varying numbers of spherical turbulators increased heat transfer by preventing the formation of the boundary layer [39]. In comparison to the turbulated pipes, the supported empty pipe has a larger heat entropy production rate, but a lower friction entropy production rate.

Temperature-induced entropy production rate was reduced by expanding the quantity of spherical turbulators. The supported hollow pipe's thermal entropy production rate was computed to be between 0.072 and 0.041 $W.m^{-1}.K^{-1}$. The greatest thermally induced entropy production rate was discovered to be 0.058–0.034 $W.m^{-1}.K^{-1}$ for a single sphere turbulator, whilst the lowest was determined to be in the range of 0.039–0.023 $W.m^{-1}.K^{-1}$ for three sphere turbulators. In comparison to

the supported empty pipe, the thermally induced entropy generation rate of 1, 2, and 3 sphere turbulators decreased by a maximum of 24.38%, 57.21%, and 84.42%, respectively.

The rate of viscous-induced entropy formation was enhanced by increasing the number of sphere turbulators. It was discovered that the supported hollow pipe's viscous entropy production rate ranged from 0.0003023 to 0.0013891 $W.m^{-1}.K^{-1}$. The range of 0.0008331–0.0029620 $W.m^{-1}.K^{-1}$ was shown to be the lowest viscous-induced entropy production rate for single sphere turbulators, whereas 0.0012663–0.0036893 $W.m^{-1}.K^{-1}$ was the greatest rate for three sphere turbulators in the turbulator pipe. When comparing the supported straight pipe to the viscous-induced entropy generation rate of 1, 2, and 3 sphere turbulators, the largest increases were 175.63%, 231.56%, and 318.95%, respectively.

According to the results obtained from experimental data, total entropy production was calculated with Eq. (6). The graphs obtained from these calculation s are given in Fig. 9.

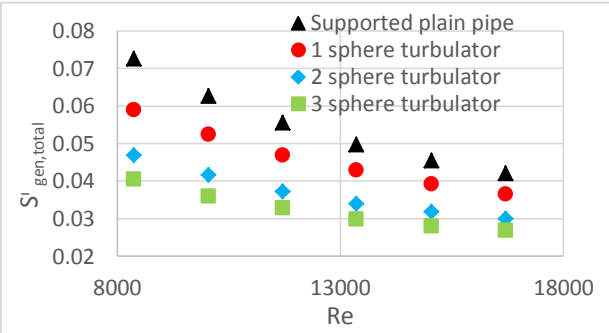

Figure 9. $S'_{gen,total}$-*Re* chart of supported plain tube and sphere turbulators

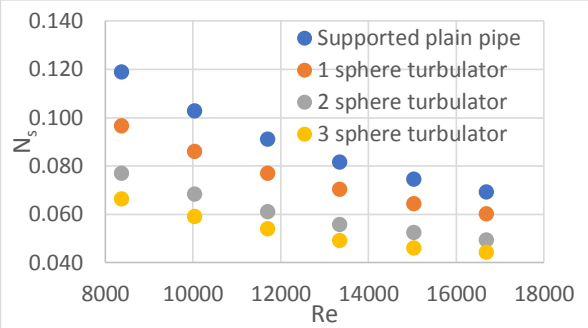

Figure 10. N_s-*Re* graph of supported plain pipe and sphere turbulators

According to Fig. 9, total entropy production graphs were similar to thermal-induced entropy production rate graphs. Thermal entropy production was more effective in total entropy production than viscous entropy production. This situation has been interpreted as irreversibility in heat transfer is greater than in friction.

According to the results obtained from experimental data, the total entropy production number was calculated with Eq. (7). The graphs obtained from these calculations are shown in Fig. 10.

As seen in Fig. 10, the total entropy production number decreased with increasing number of sphere turbulators and Reynolds number. At low Reynolds numbers, the total entropy production numbers of sphere turbulators were separated from one another; however, as Reynolds numbers climbed, this difference diminished even more. When comparing the supported empty pipe to sphere turbulators, the largest increase in total entropy production number was 1.79 times for three sphere turbulators at *Re* = 8379.

4. Conclusions

In this research, the effects of sphere turbulators placed in a circular test pipe were experimentally examined in the number range *Re* = 8379-16701, taking into account the first and second laws of thermodynamics. The results obtained are given below.

- In general, sphere turbulators placed in the test pipe increased the contact area of the fluid with the wall. Thus, the heat exchange between the test pipe under constant heat flux and the working fluid water increased.

- As a result of the increase in the number of sphere turbulators and the Reynolds number, the turbulence of the fluid increased. With increasing number of sphere turbulators, Nusselt number values, friction factor, thermal performance factor and friction-induced entropy production increased, while heat transfer-induced entropy production, total entropy production and total entropy production number decreased. Thermal entropy dominated the total entropy production.
- Compared to the supported empty pipe, the maximum Nusselt number increase was 83.34% for the test pipe with 3 sphere turbulators. The minimum and maximum Nusselt number increase rates of 3 sphere turbulators compared to 1 and 2 sphere turbulators were obtained as 42.61%-46.93% and 13.99%-17.11%, respectively.
- The increase rates of maximum friction factors of 1, 2 and 3 sphere turbulators compared to the supported empty pipe were 174.42%, 226.70% and 306.53%, respectively.
- The maximum total entropy rate for sphere turbulators was obtained as 0.058 $W.m^{-1}.K^{-1}$ for 1 sphere turbulator at $Re = 8379$.
- In terms of the second law, the maximum entropy generation of sphere turbulators compared to the supported empty pipe decreased by 79.39% for 3 sphere turbulators at $Re = 8379$.
- Compared to sphere turbulators, the maximum increase in the total entropy production number of the supported empty pipe was 1.79 times for 3 sphere turbulators at $Re = 8379$.
- Maximum Nusselt number, friction factor and *TPF* respectively; it was determined as 231.28 for $Re = 16701$ and 3 sphere turbulators, as 0.440 for $Re = 8379$ and 3 sphere turbulators, and as 1.28 for $Re = 16701$ and 3 sphere turbulators.
- According to the results of this study, it was concluded that the optimum number of sphere turbulators is 3 sphere turbulators with the lowest entropy production number and the highest *TPF* value.

In practice, it is recommended to use sphere turbulators in terms of ease of production and installation, heat transfer enhancement and thermal performance. For better heat transfer and lower friction factor, drilling holes on the sphere turbulators, creating different geometrically shaped cavities, etc. The current study can be further tested and improved with applications.

Nomenclature

A	-	Area [m^2]	u	-	Average axial velocity [$m.s^{-1}$]
C_p	-	Specific heat at constant pressure [$kj.kg^{-1}.K^{-1}$]	$x_1, ..., x_n$	-	Uncertainty regarding independent variables
D	-	Diameter [m]	Y	-	Output quantity
f	-	Friction factor	ΔP	-	Pressure drop [Pa]
ff	-	Friction factor	$\dot{S}'$	-	Entropy production [$W.m^{-1}.K^{-1}$]
f_p	-	Friction factor of pipe without turbulator	$\dot{Q}$	-	Volumetric flow rate [$m^3.s^{-1}$]
h	-	Average heat transfer coefficient [$W.m^{-2}.K^{-1}$]	ρ	-	Fluid density [$kg.m^{-3}$]
ht	-	Heat transfer	***Subscripts***		
i	-	Inlet	a	-	Pipe with turbulator
k	-	Heat conduction coefficient [$W.m^{-1}.K^{-}$	avg	-	Average

		[1]]			
Nu	-	Nusselt number (=hD/k)	*conv*	-	Convection
Nu_p	-	Nusselt number of pipe without turbulator	*gen*	-	Generation
N_s	-	Total entropy production num.	*h*	-	Hydraulic
Q	-	Heat transfer rate [W]	*o*	-	Outlet
Re	-	Reynolds number ($=\rho u D_h/\mu$)	*o*	-	Straight pipe without turbulator
T	-	Temperature [K]	*pp*	-	Pumping power
TPF	-	Termal performance factor	*w*	-	Wall

References

[1] Yao, B., *et al.*, Improving the thermal performance of the heat exchanger through simultaneous utilization of novel magnetic turbulators and helical coil wire turbulators, *International Journal of Thermal Sciences, 197* (2024), 108812, doi: 10.1016/J.IJTHERMALSCI.2023.108812

[2] Sekulic, D. P., Shah, R. K., *Fundamentals of Heat Exchanger Design*, John Wiley and Sons Inc, 2024

[3] Kakaç, S., *et al.*, *Heat Exchangers: Selection, Rating, and Thermal Design*, CRC Press, Second Edition, 2002

[4] Mashoofi, N., *et al.*, Numerical study of heat transfer and exergy loss in a double tube heat exchanger with corrugated inner tube: the new configuration of corrugated tubes, *Journal of Mechanical Engineering*, *48* (2018), 3, pp. 301-307 (in Persian)

[5] Cheraghi, M. H., *et al.*, Numerical study on the heat transfer enhancement and pressure drop inside deep dimpled tubes, *Int J Heat Mass Transf*, *147* (2020), 118845, doi: 10.1016/J.IJHEATMASSTRANSFER.2019.118845

[6] Amani, M., *et al.*, The efficacy of magnetic field on the thermal behavior of MnFe2O4 nanofluid as a functional fluid through an open-cell metal foam tube, *J Magn Magn Mater*, *432* (2017), pp. 539-547, doi: 10.1016/J.JMMM.2017.02.045

[7] Asar, F. J., *et al.*, Direct synthesis of piperazines containing dithiocarbamate derivatives via DABCO bond cleavage, *Tetrahedron Lett*, *61* (2020), 49, 152610, doi: 10.1016/J.TETLET.2020.152610.

[8] Najmi, L., Hu, Z., Effects of carbon nanotubes on thermal behavior of epoxy resin composites, *Journal of Composites Science*, *7* (2023), 8, doi: 10.3390/jcs7080313

[9] Mashoofi, N., *et al.*, Fabrication method and thermal-frictional behavior of a tube-in-tube helically coiled heat exchanger which contains turbulator, *Appl Therm Eng*, *111* (2017), pp. 1008-1015, doi: 10.1016/J.APPLTHERMALENG.2016.09.163

[10] Nakhchi, M. E., *et al.*, Effects of CuO nano powder on performance improvement and entropy production of double-pipe heat exchanger with innovative perforated turbulators, *Advanced Powder Technology*, 32 (2021), 8, pp. 3063-3074, doi: 10.1016/J.APT.2021.06.020

[11] Bahuguna, R., *et al.*, Entropy generation analysis in a tube heat exchanger integrated with triple blade vortex generator inserts, *Energy Sources, Part A: Recovery, Utilization and Environmental Effects*, 2021, doi: 10.1080/15567036.2021.1918291

[12] Maithani, R., Kumar, A., Correlations development for Nusselt number and friction factor in a dimpled surface heat exchanger tube, *Experimental Heat Transfer*, *33* (2020), 2, pp. 101-122, doi: 10.1080/08916152.2019.1573863

[13] Sheikholeslami, M., *et al.*, Heat transfer of nanoparticles employing innovative turbulator considering entropy generation, *Int J Heat Mass Transf*, *136* (2019), 1233–1240, doi: 10.1016/J.IJHEATMASSTRANSFER.2019.03.091

[14] Sepehr, M., *et al.*, Prediction of heat transfer, pressure drop and entropy generation in shell and helically coiled finned tube heat exchangers, *Chemical Engineering Research and Design*, *134* (2018), pp. 277-291, doi: 10.1016/J.CHERD.2018.04.010

[15] Farzaneh-Gord, M., *et al.*, Tube-in-tube helical heat exchangers performance optimization by entropy generation minimization approach, *Appl Therm Eng*, *108* (2016), pp. 1279-1287, doi: 10.1016/J.APPLTHERMALENG.2016.08.028

[16] Salhi, J. E., *et al.*, Numerical analysis of the properties of nanofluids and their impact on the thermohydrodynamic phenomenon in a heat exchanger, *Mater Today Proc*, *45* (2021), pp. 7559-7565, doi: 10.1016/J.MATPR.2021.02.365

[17] Salhi, J. E., *et al.*, Analysis of the thermohydrodynamic behavior of a cooling system equipped with adjustable fins crossed by the turbulent flow of air in forced convection, *International Journal of Energy and Environmental Engineering*, *13* (2022), 3, pp. 1039-1051, doi: 10.1007/s40095-021-00446-5

[18] Salhi, J. E., *et al.*, Turbulence and thermo-flow behavior of air in a rectangular channel with partially inclined baffles, *Energy Sci Eng*, 2022, doi: 10.1002/ese3.1239

[19] Salhi, J. E., *et al.*, Numerical study of the thermo-energy of a tubular heat exchanger with longitudinal baffles, *Mater Today Proc*, *45* (2021), pp. 7306-7313, doi: 10.1016/J.MATPR.2020.12.1213

[20] Fang, Y., *et al.*, Numerical study on heat and flow transfer characteristics in rectangular mini-channel with s-shaped turbulator inserted, *Thermal Science*, *27* (2023), 4, pp. 2865-2877, doi: 10.2298/TSCI220919210F

[21] Balan, V., *et al.*, Investigation on the enhancement of heat transferin counterflow double-pipe heat exchangerusing nanofluids, *Thermal Science*, *28* (2024), 1A, pp. 233-240, doi: 10.2298/TSCI230312273V

[22] Selvam, S., *et al.*, Experimental studies on effect of bonding the twisted tape with pins to the inner surface of the circular tube, *Thermal Science*, *18* (2014), 4, pp. 1273-1283, doi: 10.2298/TSCI120807036S

[23] Firat, I., *et al.*, Performance and entropy production analysis of angle blade turbulators used to increase heat transfer, *J Therm Anal Calorim*, *148* (2023), 15, pp. 7811-7828, doi: 10.1007/s10973-023-12253-7

[24] Eiamsa-ard, S., Promvonge, P., Enhancement of heat transfer in a tube with regularly-spaced helical tape swirl generators, *Solar Energy*, *78* (2005), 4, pp. 483-494, doi: 10.1016/J.SOLENER.2004.09.021

[25] Goh, L. H. K., *et al.*, Entropy generation analysis of turbulent convection in a heat exchanger with self-rotating turbulator inserts, *International Journal of Thermal Sciences*, *160* (2021), 106652, doi: 10.1016/j.ijthermalsci.2020.106652

[26] Firat, I., *et al.*, Experimental investigation of the thermal performance effects of turbulators with different fin angles in a circular pipe, *International Journal of Thermal Sciences*, *184* (2023), 107969, doi: 10.1016/J.IJTHERMALSCI.2022.107969

[27] Karagoz, S., *et al.*, Experimental investigation of the effect of wave turbulators on heat transfer in pipes, *Thermal Science*, *26* (2022), 2, pp. 1771-1783, doi: 10.2298/TSCI210206183K

[28] Kline, S. J., McClintock, F. A., Describing uncertainty in single sample experiments, *Mech. Engineering*, *75* (1953), pp. 3-8

[29] Salhi, J. E., *et al.*, Numerical investigations of the impact of a novel turbulator configuration on the performances enhancement of heat exchangers, *J Energy Storage*, *46* (2022), 103813, doi: 10.1016/J.EST.2021.103813

[30] Turgut, E., Yardımcı, U., Comprehensive analysis of the performance of the coaxial heat exchanger with turbulators, *International Journal of Thermal Sciences*, *76* (2022), 107502, doi: 10.1016/J.IJTHERMALSCI.2022.107502

[31] Ghajar, A. J., *et al.*, Experimental investigation of friction factor in the transition region for water flow in minitubes and microtubes, *Heat Transfer Engineering*, *31* (2010), 8, pp. 646-657, doi: 10.1080/01457630903466613

[32] Akyürek, E. F., *et al.*, Experimental analysis for heat transfer of nanofluid with wire coil turbulators in a concentric tube heat exchanger, *Results Phys*, *9* (2018), pp. 376-389, doi: 10.1016/J.RINP.2018.02.067

[33] Sahin, B., *et al.*, Experimental investigation of heat transfer and pressure drop characteristics of Al2O3–water nanofluid, *Exp Therm Fluid Sci*, *50* (2013), pp. 21-28, doi: 10.1016/J.EXPTHERMFLUSCI.2013.04.020

[34] Luo, J., *et al.*, Thermal-frictional behavior of new special shape twisted tape and helical coiled wire turbulators in engine heat exchangers system, *Case Studies in Thermal Engineering*, *53* (2024), 103877, doi: 10.1016/J.CSITE.2023.103877

[35] Hong, Y., *et al.*, Turbulent thermal, fluid flow and thermodynamic characteristics in a plain tube fitted with overlapped multiple twisted tapes, *Int J Heat Mass Transf*, *115* (2017), pp. 551-565, doi: 10.1016/J.IJHEATMASSTRANSFER.2017.08.017

[36] Kongkaitpaiboon, V., *et al.*, Experimental investigation of heat transfer and turbulent flow friction in a tube fitted with perforated conical-rings, *International Communications in Heat and Mass Transfer*, 37 (2010), 5, pp. 560-567, doi: 10.1016/J.ICHEATMASSTRANSFER.2009.12.015

[37] Eiamsa-ard, S., *et al.,* Convective heat transfer in a circular tube with short-length twisted tape insert, *International Communications in Heat and Mass Transfer, 36* (2009), 4, pp. 365-371, doi: 10.1016/J.ICHEATMASSTRANSFER.2009.01.006

[38] Kaood, A., Fadodun, O. G., Numerical investigation of turbulent entropy production rate in conical tubes fitted with a twisted-tape insert, *International Communications in Heat and Mass Transfer, 139* (2022), 106520, doi: 10.1016/J.ICHEATMASSTRANSFER.2022.106520

[39] Jayranaiwachira, N., *et al.,* Entropy generation and thermal performance of tubular heat exchanger fitted with louvered corner-curved V-baffles, *Int J Heat Mass Transf, 201* (2023), 123638, doi: 10.1016/J.IJHEATMASSTRANSFER.2022.123638

Received: 04.03.2024.

Revised: 07.06.2024.

Accepted: 08.07.2024.